

Electronic Supplementary Information

Exceptional CO₂ working capacity in a heterodiamine-grafted metal-organic framework

Woo Ram Lee,^a Hyuna Jo,^a Li-Ming Yang,^b Hanyeong Lee,^c Dae Won Ryu,^a Kwang Soo Lim,^a
Jeong Hwa Song,^a Da Young Min,^d Sang Soo Han,^b Jeong Gil Seo,^c Yong Ki Park,^d Dohyun
Moon^e and Chang Seop Hong^{*a}

a. Department of Chemistry, Korea University, Seoul 136-713, Korea. E-mail:

cshong@korea.ac.kr

b. Center for Computational Science, Korea Institute of Science and Technology (KIST),

Hwarangno 14-gil 5, Seongbuk-gu, Seoul 136-791, Korea.

c. Department of Energy and Biotechnology, Myongji University, Myongji-ro 116, Cheoin-gu,

Yongin, Gyeonggi-do, 449-728, Korea.

d. Center for Carbon Resources Conversion, Korea Research Institute of Chemical Technology,

Daejeon, 305-600, Korea.

e. Beamline Division, Pohang Accelerator Laboratory, Pohang, Kyungbuk 790-784, Korea.

*To whom correspondence should be addressed.

Tel.: +82 232903138. E-mail: cshong@korea.ac.kr (Chang Seop Hong)

Experimental

All chemicals and solvents in the synthesis were reagent grade and used as received. H₄dobpdc and 1-DMF were prepared according to the literature.^[S1]

[Mg₂(dobpdc)(dmen)_{1.8}(H₂O)_{0.2}] (1-dmen). A sample of fully activated **1** (100 mg, 0.31 mmol) was loaded in a Schlenk flask under a glove box. A solution of dry hexane (100 mL) with 20 equiv of N,N-dimethylethylenediamine (dmen, 0.68 mL, 6.27 mmol) was transferred to the flask using a cannula. The suspension was stirred for 18 h at room temperature. The solid was separated by filtration and washed with dry hexane several times. The resulting residue was immersed in dry hexane for 72 h and then evacuated at 130 °C for 4 h to obtain an off-white powder. Yield: 150 mg (99.5%). Elemental analysis calcd (%) for C_{21.2}H_{28.6}Mg₂N_{3.6}O_{6.4} [**1-dmen-(H₂O)**]_{0.3}: C 52.34, H 5.87, N 10.24; found: C 52.34, H 5.93, N 10.37.

Powder X-ray Diffraction and Structure Modeling. The synchrotron powder X-ray diffraction data were collected at 298K with the 240 mm of detector distance in 120 s exposure with synchrotron radiation ($\lambda = 1.10004\text{\AA}$) using a 2D SMC ADSC Quantum-210 detector with a silicon (111) double crystal monochromator at the Pohang Accelerator Laboratory. The ADX program^[S2] was used for data collection, and Fit2D program^[S3] was used for converting a two-dimensional diffraction image to a one-dimensional diffraction pattern. The unit cell dimensions of **1-dmen**, **1-dmen-CO₂**, and **1-dmen-re** were determined by conducting a full-pattern decomposition with the Le Bail method (Pawley refinement) implemented in *TOPAS-Academic*. The trigonal space group *P*3₂1 was utilized for the refinements, due to the isomorphism with Zn₂(dobpdc).^[S1] Based on the unit cell dimensions obtained, the geometry of the backbones was optimized via an energy minimization algorithm using the universal force field implemented in the *Forcite* module of *Materials Studio*.^[S4]

Gas Sorption Measurements. Gas sorption isotherms were measured using a Micromeritics ASAP2020 instrument up to 1 atm of gas pressure unless otherwise stated. The highly pure N₂ (99.999%), CO₂ (99.999%), and O₂ (99.995%) were used in the sorption experiments. N₂ gas isotherms were measured at 77 K and 298 K, and CO₂ uptake was measured at 298 K, 313 K, 323 K, 333 K, 343 K, 348 K and 363 K.

Thermogravimetric Analyses and Gas Cycling Measurements. Thermogravimetric analyses (TGA) were carried out at a ramp rate of 3 °C/min in an Ar (99.999 %) flow using a Scinco TGA N-1000 instrument. CO₂ cycling experiments were carried out on the instrument with 15% CO₂ in N₂, high purity CO₂ (99.999%), and Ar (99.999 %). A flow rate of 60 mL/min was applied for all gases. We conducted cycling experiments using a fresh sample [Mg₂(dobpdc)(dmen)_{1.8}(H₂O)_{0.2}] (**1-dmen**), in which more en was grafted onto the open metal sites, to check the N/Mg ratio.

Infrared Spectroscopy Measurements. Infrared spectra were obtained with KBr pellets and an air-tight homemade IR cell composed of KBr windows using a Bomem MB-104 spectrometer. Prior to the IR measurements, high purity N₂ (99.999 %) was purged into a sample chamber, a detector, and an IR source to remove CO₂ in air.

Other Physical Measurement. Elemental analyses for C, H, and N were performed at the Elemental Analysis Service Center of Sogang University.

DFT calculations. We calculated the stabilities and CO₂ binding energies of alkylamine functionalized MOFs by density functional theory (DFT) with van der Waals correction (called the DFT-D2^[S5] method) in the VASP^[S6] program. The three-dimensional structures of the MOFs were optimized in rhombohedral crystal structure (primitive cell) using the Perdew-Burke-Ernzerhof (PBE)^[S7] exchange-correlation functional. Valence electrons were described by a plane wave basis set with an energy cutoff of 500 eV. Due to the large size of the cell (192 atoms for the stability calculations and 390 atoms for the CO₂ binding calculations), the calculations were performed at the gamma (Γ) point.

[Reference]

- [s1] T. M. McDonald, W. R. Lee, J. A. Mason, B. M. Wiers, C. S. Hong, J. R. Long, *J. Am. Chem. Soc.* **2012**, *134*, 7056.
- [s2] A. J. Arvai, C. Nielsen, ADSC Quantum-210 ADX Program, Area Detector System Corporation; Poway, CA, USA, 1983.
- [s3] Fit2D Program: Hammersley, A. (E-mail: hammersley@esrf.fr), ESRF, 6 RUE JULES HOROWITZ BP 220 38043 GRENOBLE CEDEX 9 FRANCE.
- [s4] H. Deng, S. Grunder, K. E. Cordova, C. Valente, H. Furukawa, M. Hmadeh, F. Gandara, A. C. Whalley, Z. Liu, S. Asahina, H. Kazumori, M. O'Keeffe, O. Terasaki, J. F. Stoddart, O. M. Yaghi, *Science* **2012**, *336*, 1018-1023.
- [s5] J. Moellmann, S. Grimme, *Phys. Chem. Chem. Phys.* **2010**, *12*, 8500.
- [s6] G. Sun, J. Kürti, P. Rajczyk, M. Kertesz, J. Hafner, G. Kresse, *J. Mol. Struct. (THEOCHEM)* **2003**, *624*, 37.
- [s7] J. P. Perdew, K. Burke, M. Ernzerhof, *Phys. Rev. Lett.* **1996**, *77*, 3865.

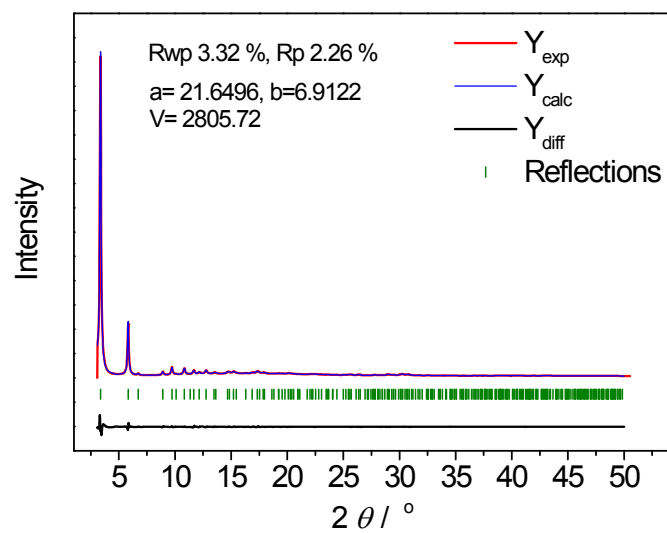


Fig. S1 Synchrotron powder X-ray diffraction pattern of **1-dmen** with calculated diffraction pattern (blue) from Pawley refinement with difference (black).

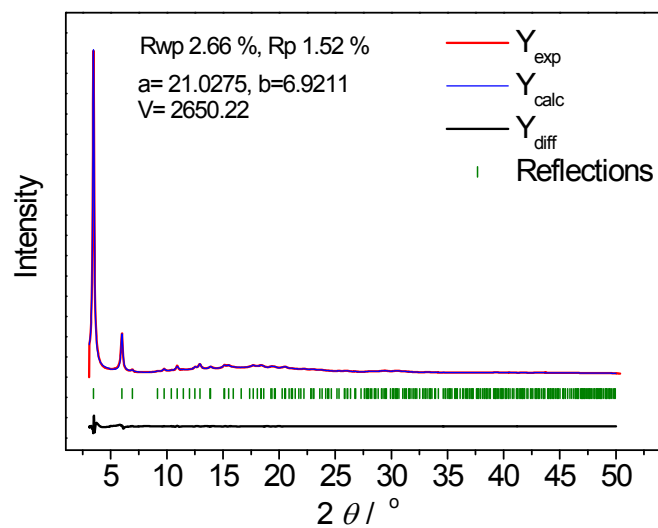


Fig. S2 Synchrotron powder X-ray diffraction pattern of **1-dmen-CO₂** with calculated diffraction pattern (blue) from Pawley refinement with difference (black).

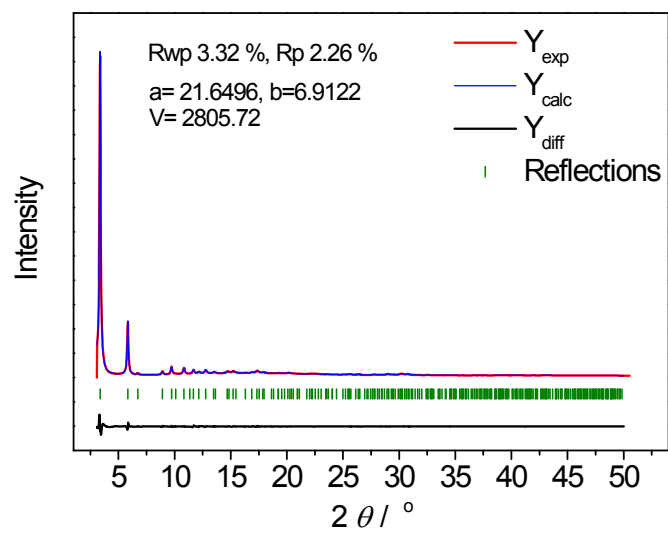


Fig. S3 Synchrotron powder X-ray diffraction pattern of **1-dmen-re** with calculated diffraction pattern (blue) from Pawley refinement with difference (black).

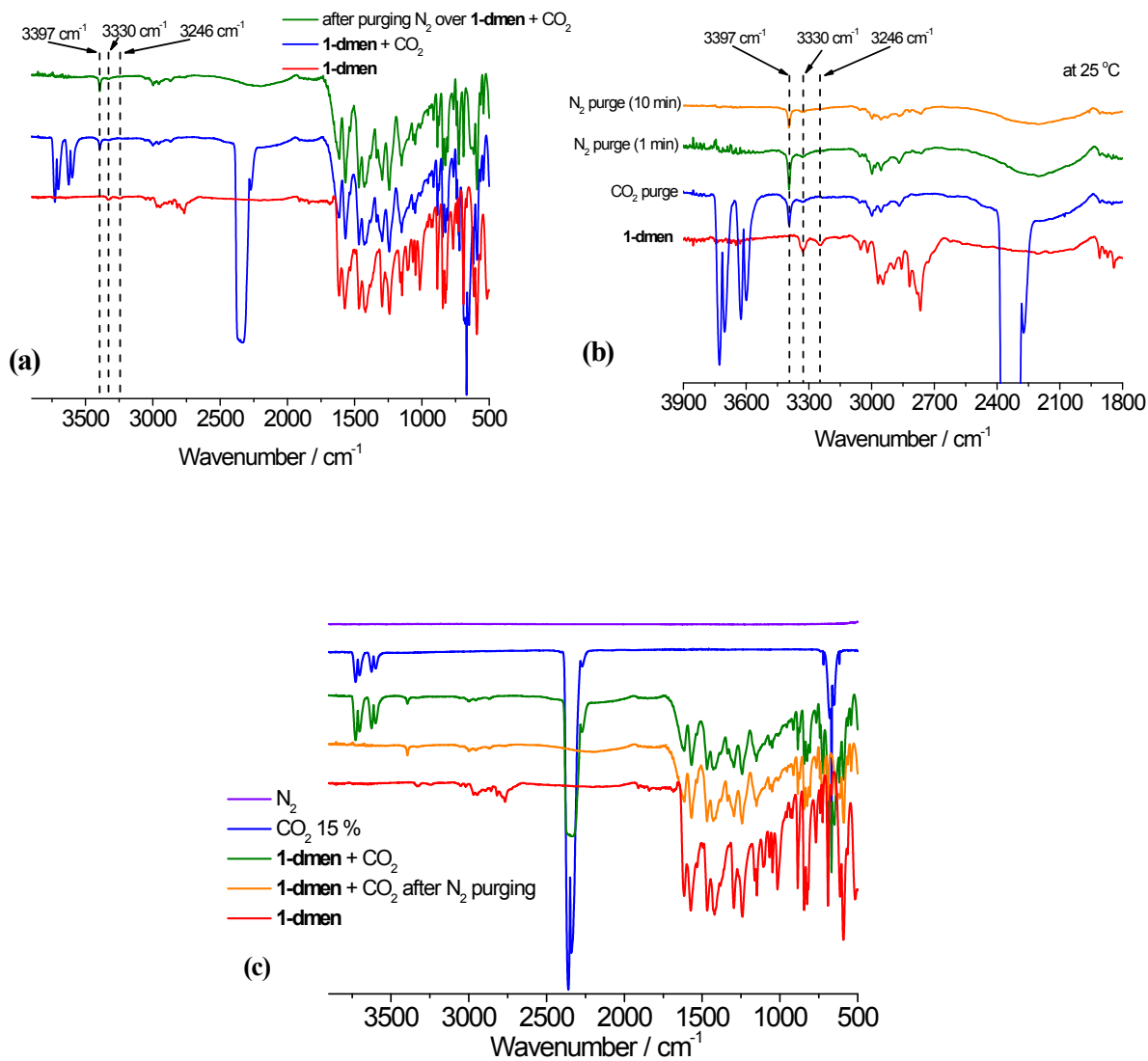


Fig. S4 (a) In-situ IR data of **1-dmen**, **1-dmen** under flowing CO₂, followed by an N₂ purge for 1 min. (b) Enlarged diagram with additional spectrum after 10 min N₂ purge. (c) IR spectra of pure N₂ and 15% CO₂. The IR data can be compared with those of the other samples. We used an air-tight IR cell (KBr windows) and an oil bubbler to isolate the cell atmosphere from air.

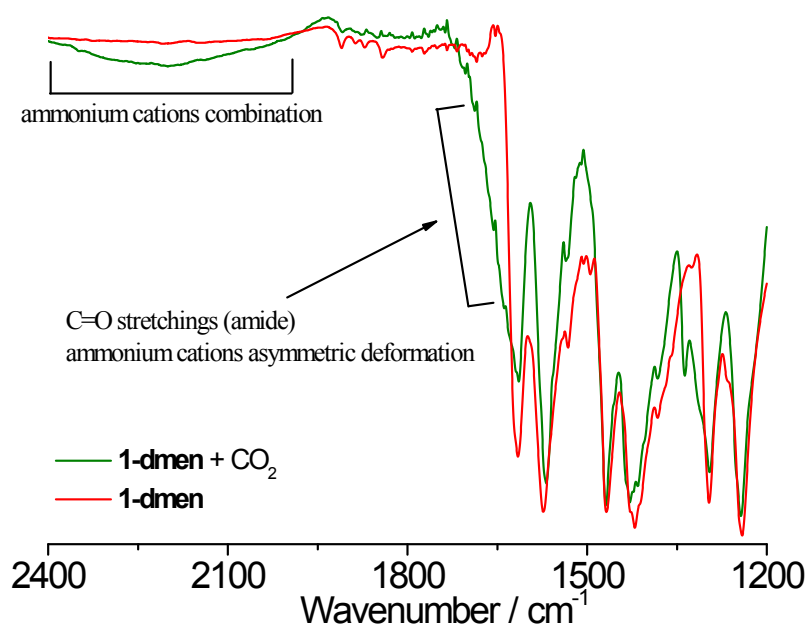


Fig. S5 Enlarged view of in-situ IR data of **1-dmen** and **1-dmen**+CO₂ in the wavenumber range 2400 -1200 cm⁻¹.

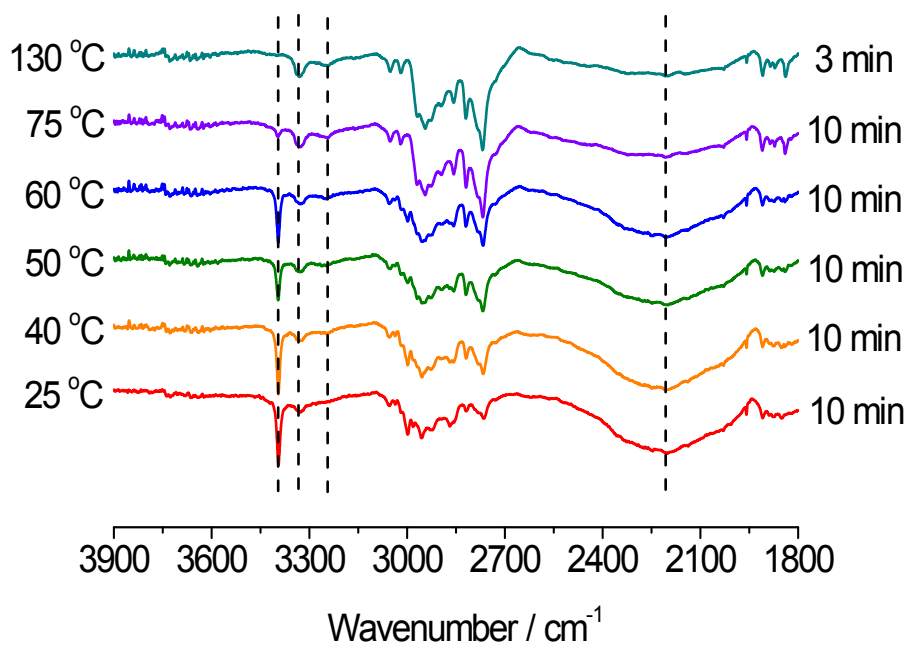


Fig. S6 In-situ IR data of **1-dmen** as a function of temperature. The sample was heated up to the set temperature under flowing CO₂. After the set temperature arrived, pure N₂ was flowed over the sample for 10 min and then the IR spectrum was taken. The spectrum of **1-dmen** at 130 °C was obtained by purging N₂ for 3 min.

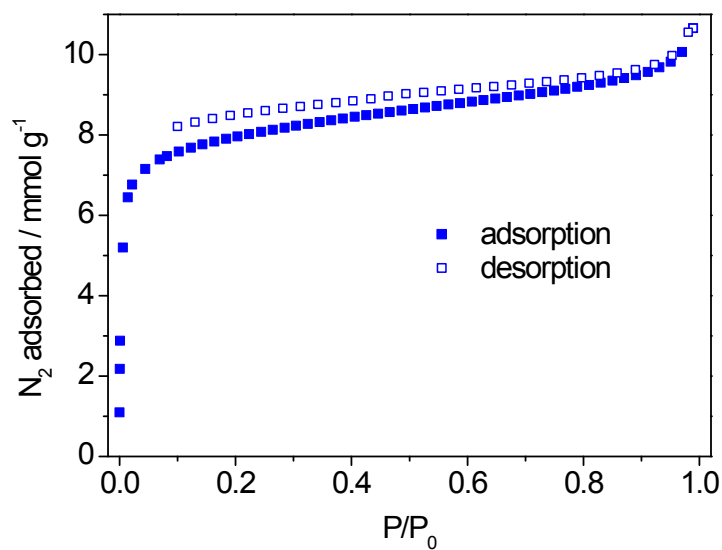


Fig. S7 N₂ isotherm of **1-dmen** at 77 K.

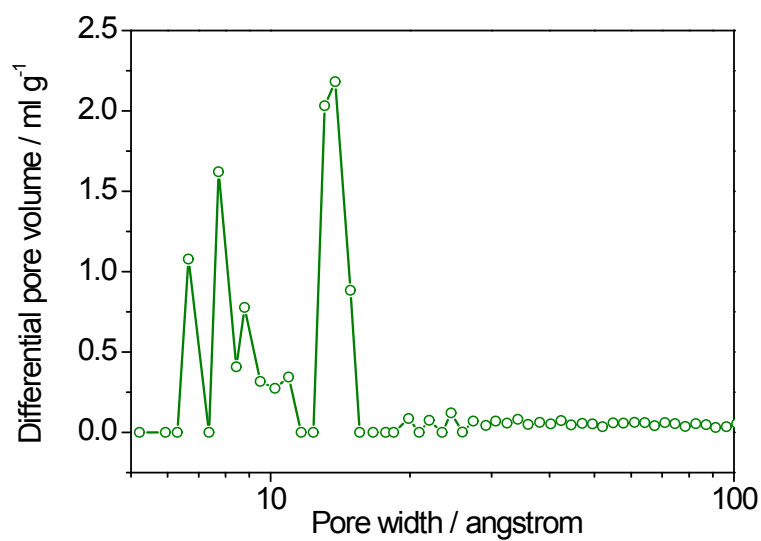


Fig. S8 DFT pore size distribution for **1-dmen** calculated from N₂ adsorption at 77 K using a Tarazona NLDFT with a cylinder pore geometry.

Isosteric Heats of Adsorption Calculations. We used a dual-site Langmuir-Freundlich equation to model the CO₂ uptake in the range before the step in the isotherms at 40, 50, and 60 °C for **1-dmen**.

$$q = \frac{q_{\text{sat,A}} b_A p^{\alpha_A}}{1 + b_A p^{\alpha_A}} + \frac{q_{\text{sat,B}} b_B p^{\alpha_B}}{1 + b_B p^{\alpha_B}}$$

Here, q denotes the amount of CO₂ adsorbed (mmol/g), p the pressure (bar), q_{sat} the saturation amount (mmol/g), b the Langmuir-Freundlich parameter (bar^{- α}), and α the Langmuir-Freundlich exponent (dimensionless) for two adsorption sites A and B. A modified Langmuir-Freundlich equation was utilized to model the CO₂ uptake in the region after the step.

$$q = \frac{q_{\text{sat,A}} b_A (p - p_{\text{step}})^{\alpha_A}}{1 + b_A (p - p_{\text{step}})^{\alpha_A}} + \frac{q_{\text{sat,B}} b_B (p - p_{\text{step}})^{\alpha_B}}{1 + b_B (p - p_{\text{step}})^{\alpha_B}} + \frac{q_{\text{sat,C}} b_C (p - p_{\text{step}})^{\alpha_C}}{1 + b_C (p - p_{\text{step}})^{\alpha_C}}$$

Here, adsorption sites are considered at A, B, and C, and an extra parameter, p_{step} , are employed to express the pressure of the step in the isotherm. We carefully refined the parameters in equations above and obtained good agreement between the experimental data and the corresponding fits. The isotherm fits were used to determine the exact pressures, p , corresponding to constant amounts of CO₂ adsorbed, q , at 40, 50, and 60 °C. The Clausius-Clapeyron equation was then utilized to extract the isosteric heats of adsorption (Q_{st}).

$$(\ln p)_q = \left(\frac{Q_{\text{st}}}{R} \right) \left(\frac{1}{T} \right) + C$$

Table S1 Dual-Site Langmuir-Freundlich parameters for the pre-step region of the CO₂ adsorption isotherm for **1-dmen** at 40°C, 50 °C and 60°C. (activated at 75 °C)

	40°C	50°C	60°C
$q_{\text{sat, A}} / \text{mmol g}^{-1}$	0.00137	0.03225	12.49719
$b_{\text{A}} / \text{bar}^{-a}$	2.78534E-14	0.71669	8.70554E-12
α_{A}	2.81291E-8	7.49588E-14	3.46504
$q_{\text{sat, B}} / \text{mmol g}^{-1}$	1.44123	1.51477	0.43774
$b_{\text{B}} / \text{bar}^{-a}$	5.53749E-4	1.5886E-5	0.00108
α_{B}	1.07006	1.63082	0.9544

Table S2 Modified dual-Site Langmuir-Freundlich parameters for the post-step region of the CO₂ adsorption isotherm for **1-dmen** at 40°C, 50 °C and 60°C. (activated at 75 °C)

	40°C	50°C	60°C
P_{step}	73.4152	196.422	416.44
$q_{\text{sat, A}} / \text{mmol g}^{-1}$	3.67257	1.04206	7.51705
$b_{\text{A}} / \text{bar}^{-a}$	1.03001	1.72384	0.08931
α_{A}	0.37048	101.62918	0.1661
$q_{\text{sat, B}} / \text{mmol g}^{-1}$	2.67847	2.96609	1.85213
$b_{\text{B}} / \text{bar}^{-a}$	9.75879E-7	0.29909	0.05081
α_{B}	1.93223	0.42514	1.84653
$q_{\text{sat, C}} / \text{mmol g}^{-1}$	8.86088E-9	0.62056	0.01567
$b_{\text{C}} / \text{bar}^{-a}$	7.63196E-11	3.51892E-7	6.33778E-5
α_{C}	4.43609E-5	2.12354	2.37025

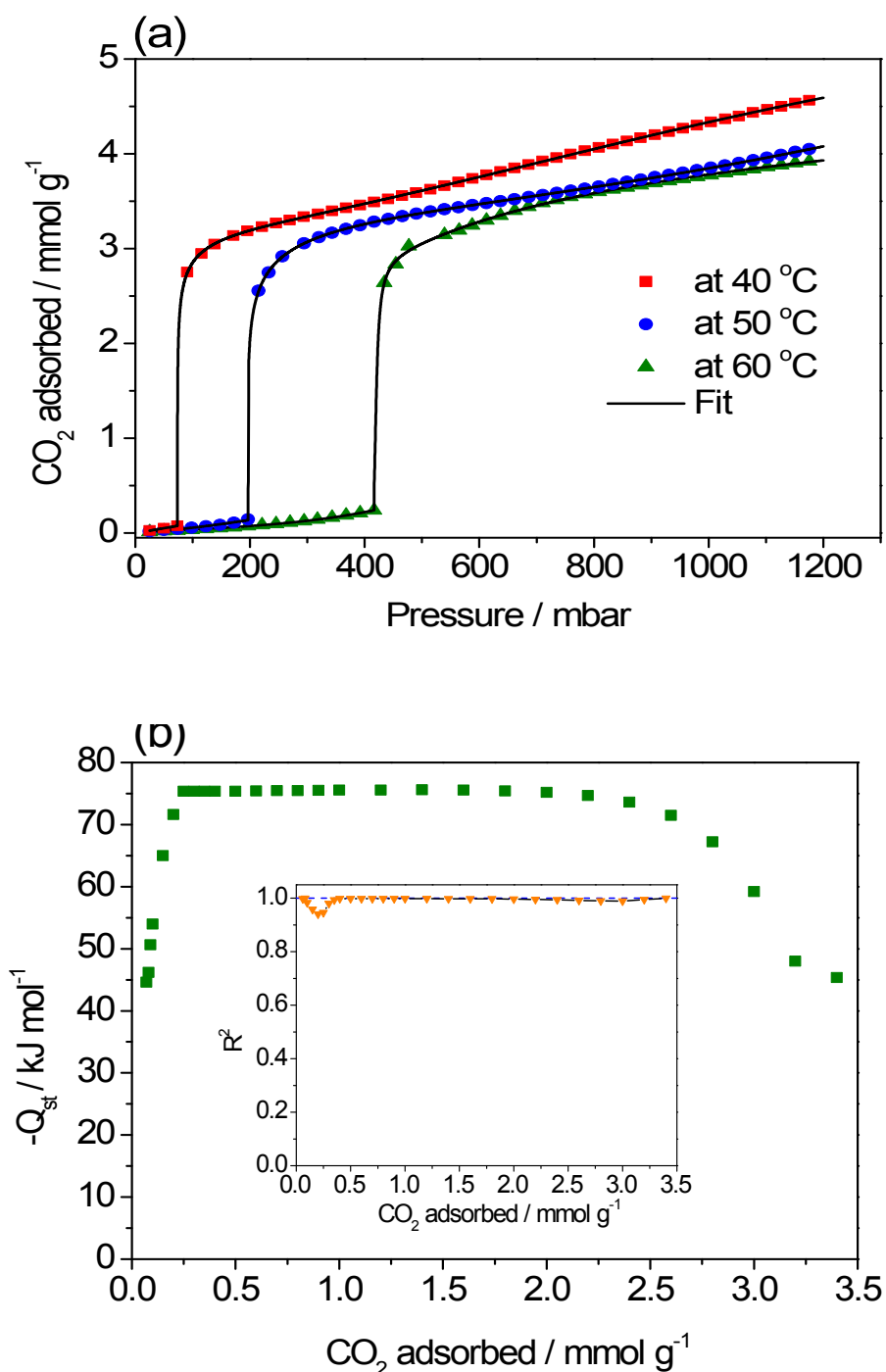


Fig. S9 (a) CO₂ isotherms and fits based on a dual-site Langmuir-Freundlich equation for **1-dmen** at 40, 50, and 60°C. (b) Isosteric heats of CO₂ adsorption for **1-dmen**, as calculated using the Clausius-Clapeyron relation. The inset indicates residual sum of squares (R²) for the best fit line of ln p versus 1/T as a function of the constant CO₂ loading used in the Clausius-Clapeyron equation.

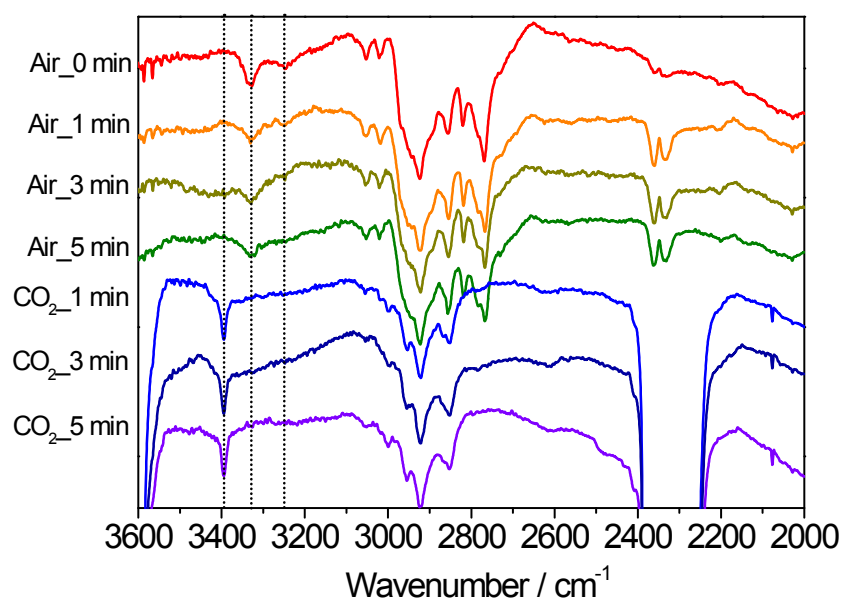
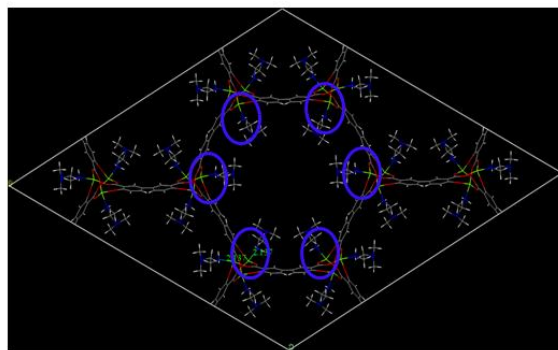


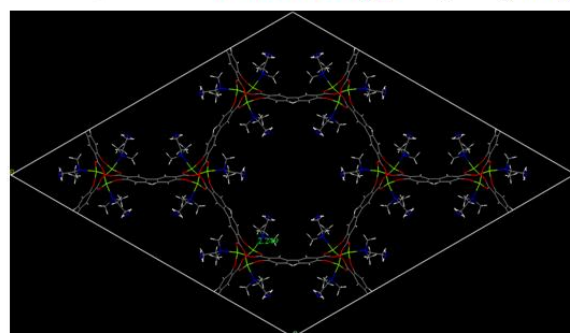
Fig. S10 Time-dependent in-situ IR data of **1-dmen** after flowing 0.39 mbar (simulated air) or pure CO₂ at 40 °C. We used an air-tight IR cell (KBr windows) and an oil bubbler to isolate the cell atmosphere from air.

Configuration 1: $\text{Mg-NH}_2\text{-CH}_2\text{-CH}_2\text{-N(CH}_3)_2$



$$E_{\text{bind}} = -174.3 \text{ kJ/mol per amine}$$

Configuration 2: $\text{Mg-N(CH}_3)_2\text{-CH}_2\text{-CH}_2\text{-NH}_2$



$$E_{\text{bind}} = -135.6 \text{ kJ/mol per amine}$$

Fig. S11 Possible binding modes of dmen to the open metal sites of **1**, performed by DFT calculations.

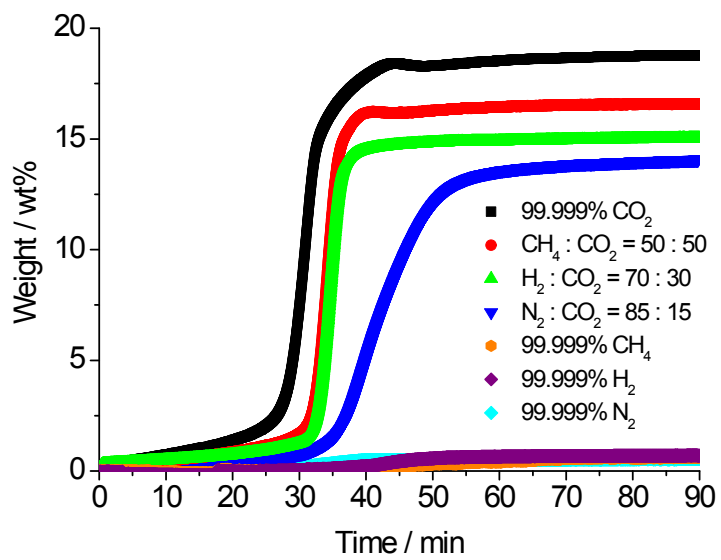


Fig. S12 Time-dependent gas uptake curves of **1-dmen** under the indicated gas mixtures at 40 °C.

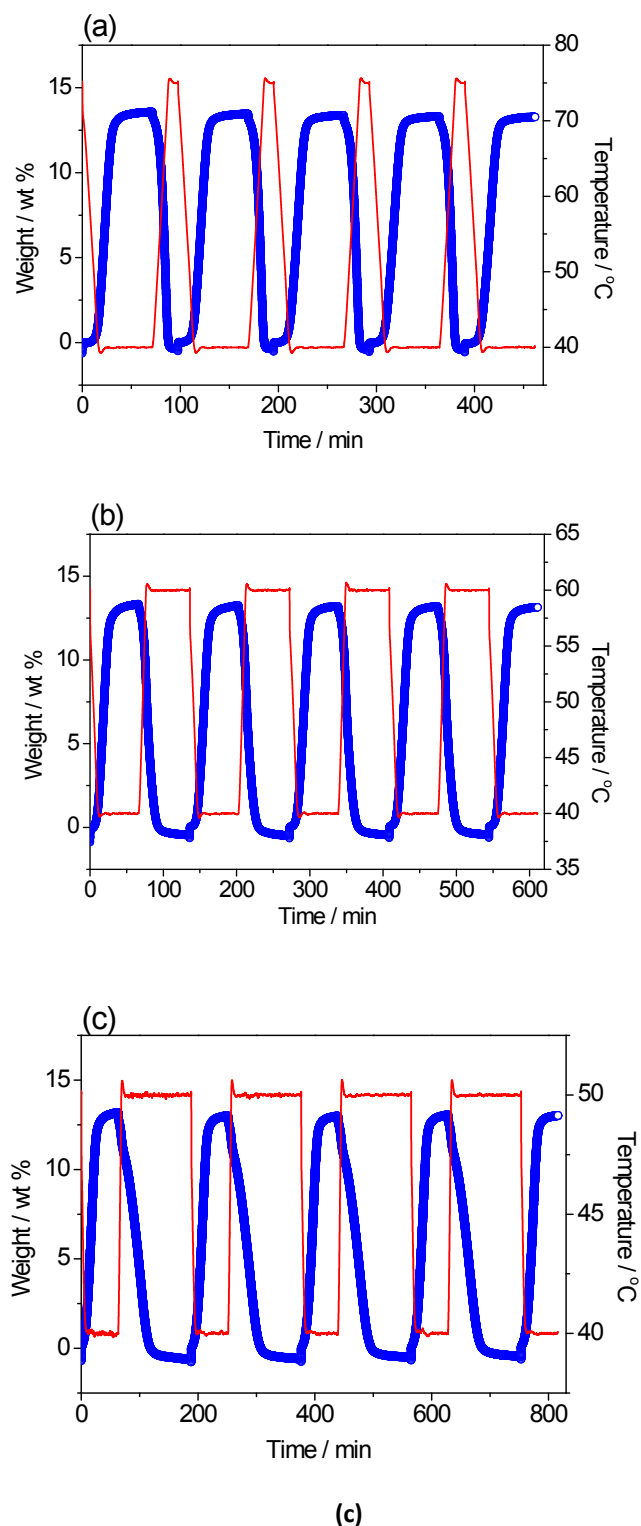


Fig. S13 Adsorption-desorption cycling of CO₂ for **1-dmen**, showing reversible uptake from simulated flue gas (0.15 bar CO₂ balanced with N₂). Adsorption temperature was 40 °C, and desorption temperature was (a) 75°C (desorption time = 10 min), (b) 60 °C (desorption time = 1 h), and (c) 50 °C (desorption time = 2 h) under flowing Ar.

In-situ IR spectroscopy as a function of time. After CO₂ was allowed to flow over the sample at the given temperature, N₂ was purged for several minutes. The IR data at 40 °C show that the N-H peak progressively disappears while the primary N-H peaks are enhanced. The same feature was observed at higher temperatures although the N-H fades out more rapidly. It is interesting to note that the adsorbed CO₂ can be desorbed even at 40 °C when N₂ is purged long enough.

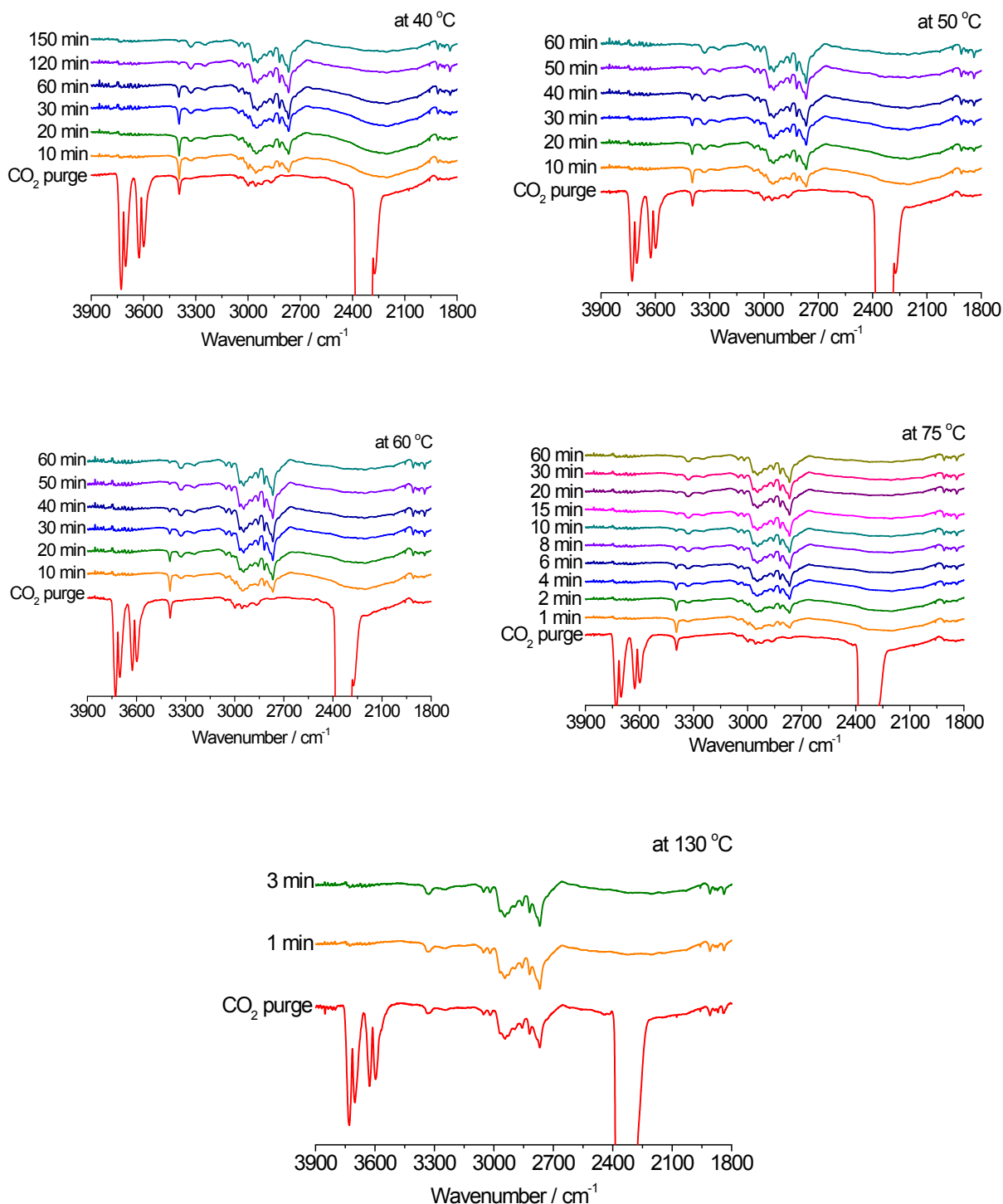


Fig. S14 In-situ IR data of **1-dmen** as a function of time. The sample was heated up to the set temperature under flowing CO₂. After the set temperature arrived, N₂ (99.999%) was flowed over the sample for the indicated time and then the IR spectrum was taken.

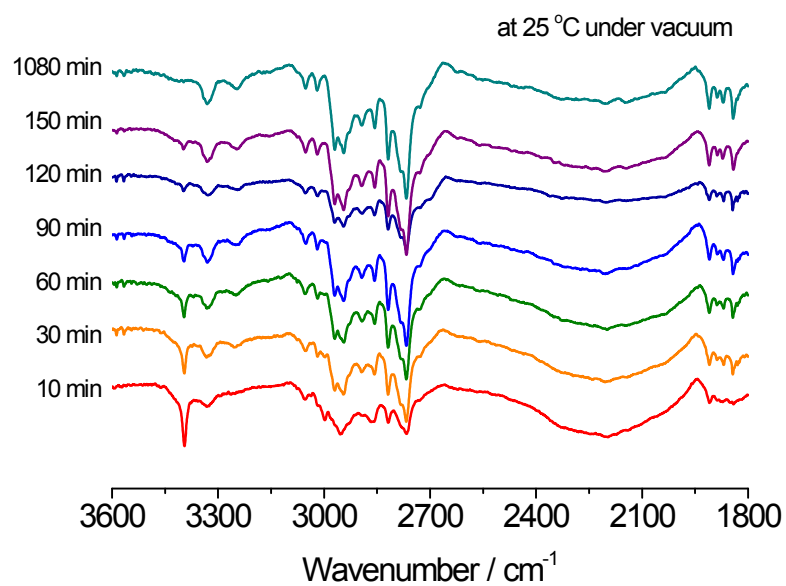


Fig. S15 In-situ IR data of **1-dmen** under vacuum. The sample was evacuated for the indicated minutes and then the IR spectrum was obtained. The broad band around 2200 cm^{-1} disappeared only in vacuum. It is noted that the N-H peak from chemisorbed species vanished at the same time.

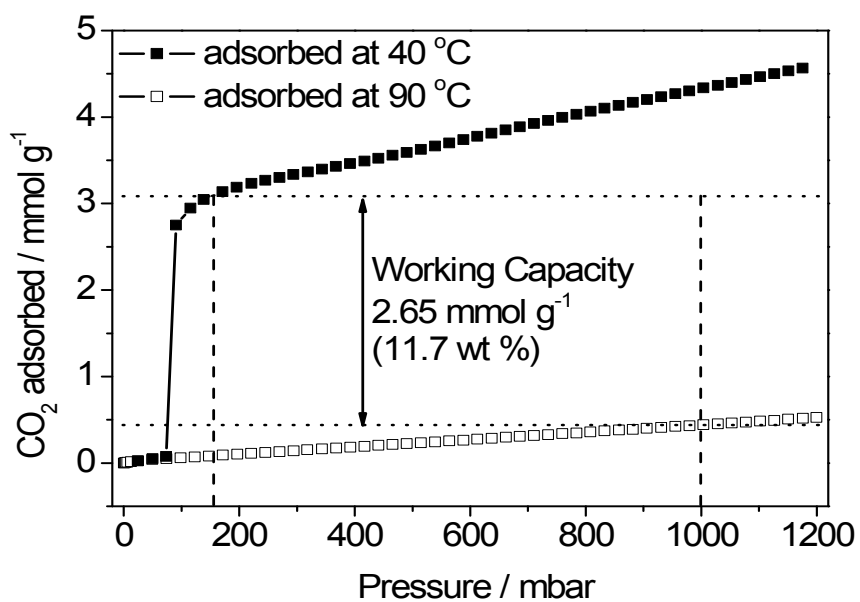
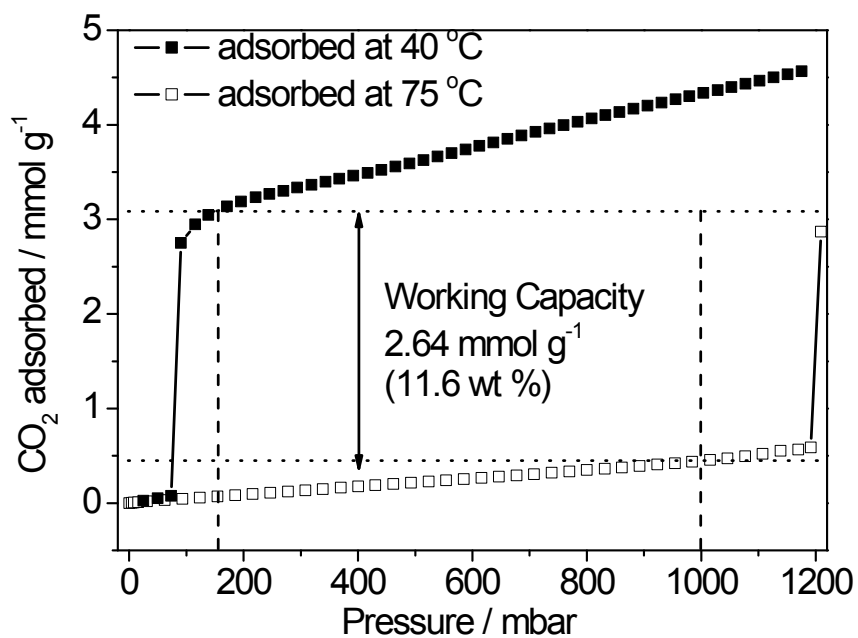


Fig. S16 Estimated working capacity from $q_{\text{ads}}(P_{\text{ads}} = 0.15 \text{ bar CO}_2, T_{\text{ads}} = 40 \text{ °C}) - q_{\text{des}}(P_{\text{des}} = 1 \text{ bar CO}_2, T_{\text{des}} = 75 \text{ °C})$ (top) and 90 °C (bottom)) of **1-dmen**.

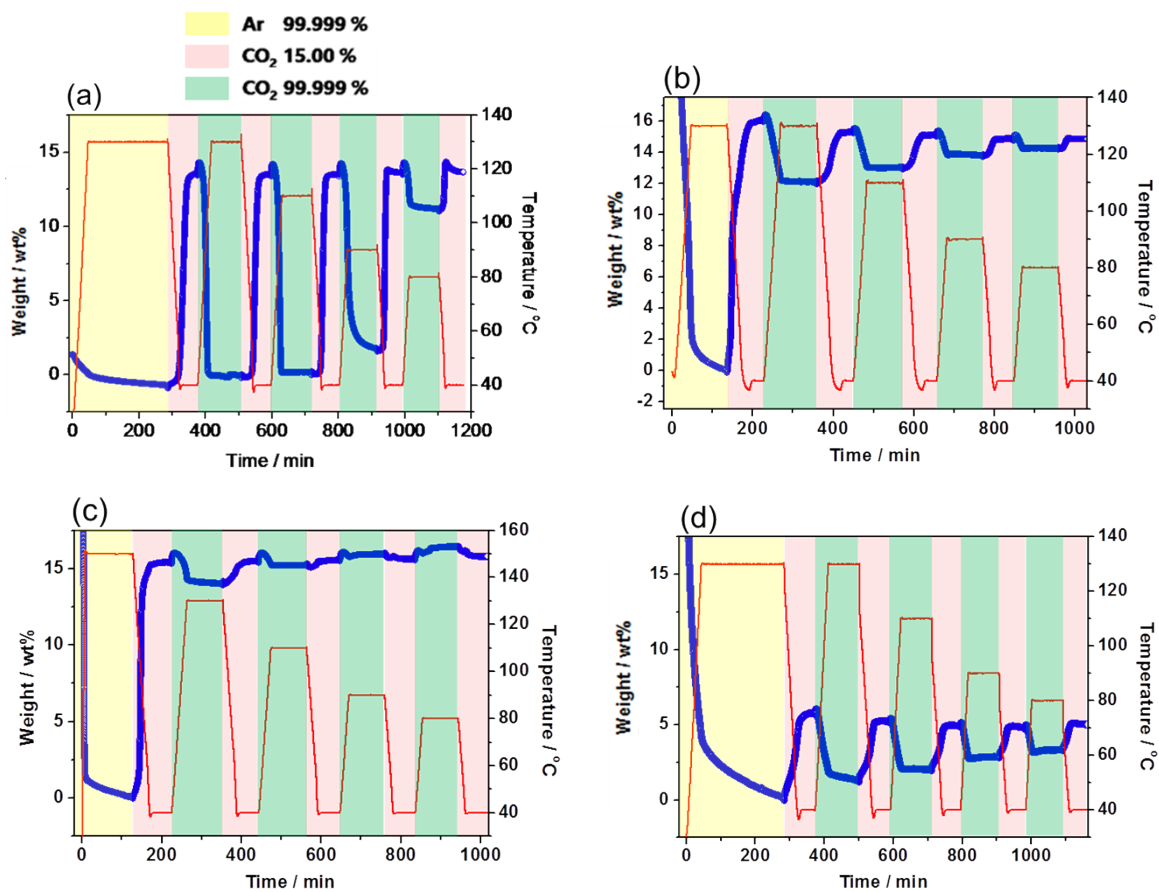


Fig. S17 TGA data for (a) **1-dmen**, (b) en-Mg₂(dobpdc), (c) mmen-Mg₂(dobpdc), and (d) tmen-Mg₂(dobpdc) in the temperature-swing adsorption process. The sample was activated at 130, 110, 90 and 80 °C under flowing pure CO₂ and then exposed to 15% CO₂ at 40 °C for the adsorption cycle. The working capacity was estimated by reading the amount adsorbed at 40 °C.

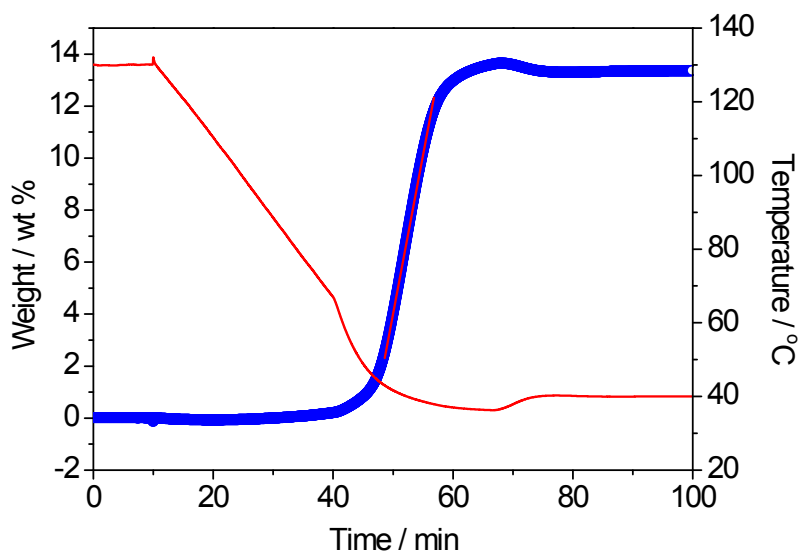


Fig. S18 Time-dependent CO₂ adsorption of **1-dmen**. Sample activation was performed under flowing pure CO₂ and adsorption under 15% CO₂. The linear fit of the adsorption curve gives an initial rate of adsorption of 1.7 wt%/min.

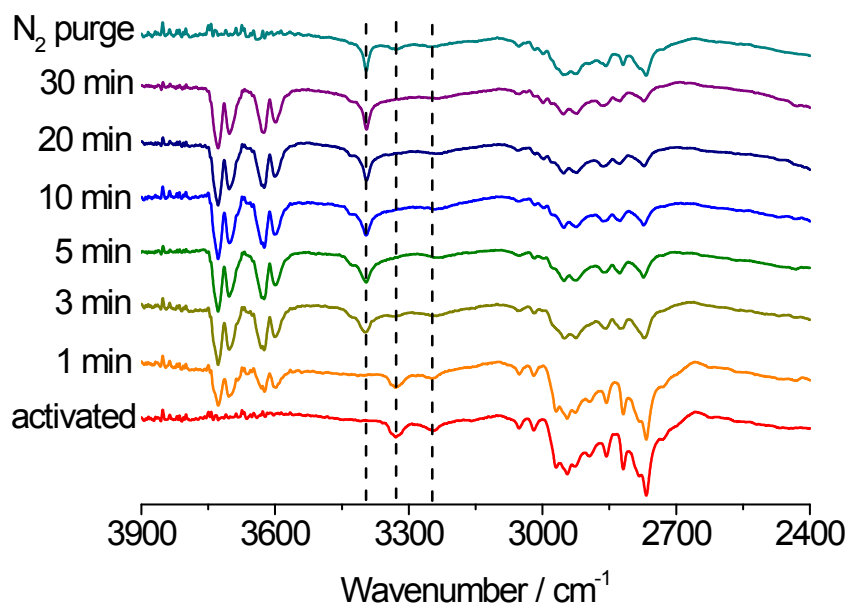


Fig. S19 Time-dependent in-situ IR data of **1-dmen** under 15% CO₂ mixed gas and 100% relative humidity (RH). We used an air-tight IR cell (KBr windows) and an oil bubbler to isolate the cell atmosphere from air. Water vapor was generated by bubbling water with 15% CO₂ and flowed into the IR cell.

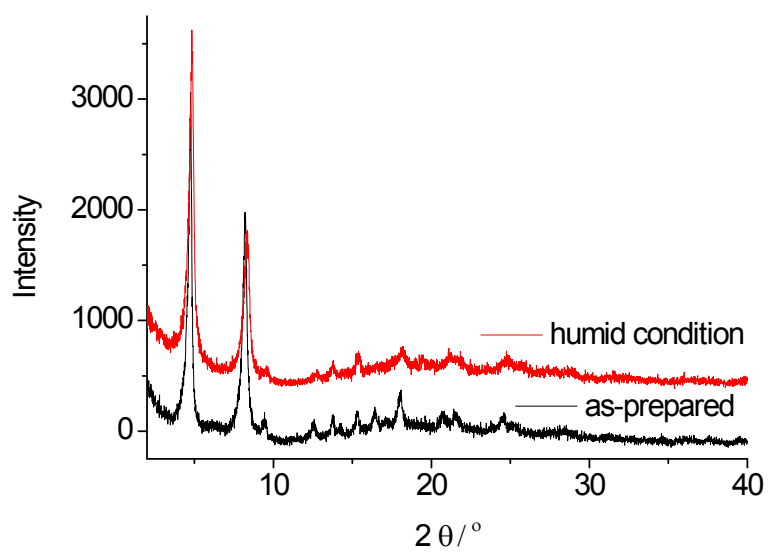


Fig. S20 PXR D patterns of the as-prepared sample (black) and the sample (red) after adsorption-desorption cycling experiments in humid conditions.